

Supplement Information

Supplementary Methods

The ODEs of the dynamic model

1) The generation and repair of DSBs:

The number of DSBs is raised during irradiation phase arise, and the number can be described as follow:

$$\frac{d[D_t]}{dt} = k_t \times a_{ir} \times IR \quad (S1)$$

$$[D(k)] = [D_1(k)] + [D_2(k)] \quad (S2)$$

$$[C(k)] = [C_1(k)] + [C_2(k)] \quad (S3)$$

$$[F(k)] = [F_1(k)] + [F_2(k)] \quad (S4)$$

$$\frac{d[D_1]}{dt} = a_1[D_t] + k_{cd1}[C_1] - (k_{dc1}[D_1] + k_{cross}([D_1] + [D_2])) \quad (S5)$$

$$\frac{d[D_2]}{dt} = a_2[D_t] + k_{cd2}[C_2] - (k_{dc2}[D_2] + k_{cross}([D_1] + [D_2])) \quad (S6)$$

$$\frac{d[C_1]}{dt} = k_{dc1}[D_1] - k_{cd1}[C_1] - k_{cf1}[C_1] \quad (S7)$$

$$\frac{d[C_2]}{dt} = k_{dc2}[D_2] - k_{cd2}[C_2] - k_{cf2}[C_2] \quad (S8)$$

$$\frac{d[F_1]}{dt} = k_{cf1}[C_1] \quad (S9)$$

$$\frac{d[F_2]}{dt} = k_{cf2}[C_2] \quad (S10)$$

The Eqs. (S1) describes the generation of DSBs under stress, Eqs. (S2)- (S4) represents the two repair process, Eqs. (S5)- (S10) shows the dynamic process among intact DSB, DSB complex and fixed DSB in repair processes, subscripts 1 and 2 describe the fast and the slow kinetics, respectively.¹⁻³

2) The self-feedback loop of ATM activation:

$$\frac{d[ATMd]}{dt} = \frac{1}{2}k_{dim}[ATM]^2 - k_{undim}[ATMd] \quad (S11)$$

$$\frac{d[ATM]}{dt} = 2k_{undim}[ATMd] - k_{dim}[ATM]^2 - k_{af}f[ATM] + k_{ar}[ATMa] \quad (S12)$$

$$\frac{d[ATMa]}{dt} = k_{af}f[ATM] - k_{ar}[ATMa] \quad (S13)$$

$$f(c,[ATMa]) = b_1c + b_2c[ATMa] + b_3[ATMa] \quad (S14)$$

Eqs. (S11)-(S14) represent the activation of ATM protein by DSBCs (obtained from the simulations described in DSBs generation and repair module). We define *ATMd*, *ATM* and *ATMa* as the concentrations of ATM dimer, inactive ATM monomer, and active ATM monomer, respectively.

In addition, we assume the total concentration of ATM molecules is a constant value, which means the equation $[ATMt] = 2[ATMd] + [ATM] + [ATMa]$ is existed, where *ATMt* represents the concentration of all forms of ATM in the cell. Therefore, the functional dependence between the number of DSBCs and [ATMa] at steady can be solved analytically.²

3) p53 regulatory network

Table S1 Variables of the p53 regulatory network

Variable	Description
mp53	p53 transcript
p53	inactive form of p53 protein
p53a	active form of p53 protein
mMdm2	Mdm2 transcript
Mdm2	inactive form of Mdm2 protein
Mdm2a	active form of Mdm2 protein
mMyc	c-Myc transcript
Myc	active form of c-Myc protein
mMucin1	Mucin1 transcript
Mucin1	active form of Mucin1 protein
cdk2	inactive form of Cyclin E/cdk2 protein
cdk2a	active form of Cyclin E/cdk2 protein
Akt	inactive form of Akt protein
Akta	active form of Akt protein

PIP2	inactive form of PIP3 protein
PIP3	active form of PIP3 protein
p21	active form of p21 protein
PTEN	active form of PTEN protein
Siah-1	active form of Siah-1 protein
miR-145	active form of miR-145 protein
ARF	active form of P19/14ARF protein
betaC	active form of Beta-Catenin protein
ATMa	active form of ATM monomer protein

p53 transcript, $mp53$: The first term stands for spontaneous p53 mRNA synthesis, while the second one describes its spontaneous degradation

$$\frac{d[mp53]}{dt} = \sigma_x - \delta_x [mp53] \quad (S15)$$

Inactive p53, $p53$: The first term stands for spontaneous $mp53$ transcription, the second one represents dephosphorylation by $p53a$, the third term represents $p53$ phosphorylation catalyzed by $ATMa$, the next two terms describes $Mdm2a$ driven and its spontaneous degradation

$$\begin{aligned} \frac{d[p53]}{dt} = & k_{xb}[mp53] + k_{cb} \frac{[p53a]}{[p53a] + J_{cb}} - k_{ab}[ATMa] \frac{[p53]}{[p53] + J_{ab}} \\ & - k_{hb}[Mdm2a] \frac{[p53]}{[p53] + J_{hb}} - \delta_b [p53] \end{aligned} \quad (S16)$$

Active p53, $p53a$: The first term describes $p53$ phosphorylation catalyzed by $ATMa$, the second one stands for $Mdm2a$ driven $p53a$ degradation, the next one represents $p53a$ dephosphorylation, and the last term stands for its spontaneous degradation

$$\begin{aligned} \frac{d[p53a]}{dt} = & k_{ab}[ATMa] \frac{[p53]}{[p53] + J_{ab}} - k_{hc}[Mdm2a] \frac{[p53a]}{[p53a] + J_{hc}} \\ & - k_{cb} \frac{[p53a]}{[p53a] + J_{cb}} - \delta_c [p53a] \end{aligned} \quad (S17)$$

Mdm2 transcript, $mMdm2$: The first term stands for spontaneous Mdm2 mRNA synthesis, the second one represents $p53a$ driven $Mdm2$ activation, and the last one describes its spontaneous degradation

$$\frac{d[mMdm2]}{dt} = \sigma_f + k_{cf} \frac{[p53a]^{nf}}{[p53a]^{nf} + J_{cf}^{nf}} - \delta_f [mMdm2] \quad (S18)$$

Inactive Mdm2, *Mdm2*: The first term stands for spontaneous *mMdm2* transcription, the second term describes driven *Mdm2a* dephosphorylation catalyzed by *ARF*, the third one represents *Mdm2a* dephosphorylation, the fourth one stands for *cdk2a* inhibited *Mdm2* phosphorylation, the next two terms represent *Akta* driven *Mdm2* and its spontaneous degradation

$$\begin{aligned} \frac{d[Mdm2]}{dt} = & k_{fg} [mMdm2] + k_{qh} [ARF] \frac{[Mdm2a]}{[Mdm2a] + J_{qh}} \\ & + k_{hg} \frac{[Mdm2a]}{[Mdm2a] + J_{hg}} - k_{kg} \frac{[Mdm2]}{[cdk2a] + J_{kg}} \\ & - k_{eg} [Akta] \frac{[Mdm2]}{[Mdm2] + J_{eg}} - \delta_g [Mdm2] \end{aligned} \quad (S19)$$

Activate Mdm2, *Mdm2a*: The first term stands for *Mdm2* phosphorylation catalyzed by *Akta*, the second one describes *Mdm2* phosphorylation inhibited by *cdk2a*, the next two terms represent itself and *ARF* driven *Mdm2a* dephosphorylation and the last two terms describe *ATMa* driven *Mdm2a* and its spontaneous degradation

$$\begin{aligned} \frac{d[Mdm2a]}{dt} = & k_{eg} [Akta] \frac{[Mdm2]}{[Mdm2] + J_{eg}} + k_{kg} \frac{[Mdm2]}{[cdk2a] + J_{kg}} \\ & - k_{hg} \frac{[Mdm2a]}{[Mdm2a] + J_{hg}} - k_{qh} [ARF] \frac{[Mdm2a]}{[Mdm2a] + J_{qh}} \\ & - k_{ah} [ATMa] \frac{[Mdm2a]}{[Mdm2a] + J_{ah}} - \delta_h [Mdm2a] \end{aligned} \quad (S20)$$

c-Myc transcript, *mMyc*: The first term stands for spontaneous c-Myc mRNA synthesis, while the second one describes its spontaneous degradation

$$\frac{d[mMyc]}{dt} = \sigma_l - \delta_l [mMyc] \quad (S21)$$

Active c-Myc, *Myc*: The first term stands for *miR-145* inhibited *Myc* transcription, and the last one stands for its spontaneous degradation

$$\frac{d[Myc]}{dt} = k_{il} \frac{[mMyc]}{[miR-145]+J_{il}} - \delta_m [Myc] \quad (S22)$$

Mucin1 transcript, *mMucin1*: The first term stands for spontaneous Mucin1 mRNA synthesis, while the second one describes its spontaneous degradation

$$\frac{d[mMucin1]}{dt} = \sigma_n - \delta_n [mMucin1] \quad (S23)$$

Active Mucin1, *Mucin1*: The first term stands for *miR-145* inhibited *mMucin1* transcription, and the last one stands for its spontaneous degradation

$$\frac{d[Mucin1]}{dt} = k_{in} \frac{[mMucin1]}{[miR-145]+J_{in}} - \delta_o [Mucin1] \quad (S24)$$

Inactive Cyclin E/cdk2, *cdk2*: The first term stands for spontaneous *cdk2* synthesis, the second one describes *cdk2a* dephosphorylation, the third one represents *cdk2a* dephosphorylation catalyzed by *p21*, the next term describes *cdk2* phosphorylation, and the last one stands for its spontaneous degradation

$$\begin{aligned} \frac{d[cdk2]}{dt} = & \sigma_j + k_{kj} \frac{[cdk2a]}{[cdk2a]+J_{kj}} + k_{pj} [p21] \frac{[cdk2a]}{[cdk2a]+J_{pj}} \\ & - k_{jk} \frac{[cdk2]}{[cdk2]+J_{jk}} - \delta_j [cdk2] \end{aligned} \quad (S25)$$

Active Cyclin E/cdk2, *cdk2a*: The first term stands for *cdk2* phosphorylation, the second one represents *cdk2a* dephosphorylation catalyzed by *p21*, the third term describes *cdk2a* dephosphorylation, and the last one stands for its spontaneous degradation

$$\begin{aligned} \frac{d[cdk2a]}{dt} = & k_{jk} \frac{[cdk2]}{[cdk2]+J_{jk}} - k_{pj} [p21] \frac{[cdk2a]}{[cdk2a]+J_{pj}} \\ & - k_{kj} \frac{[cdk2a]}{[cdk2a]+J_{kj}} - \delta_k [cdk2a] \end{aligned} \quad (S26)$$

Inactive Akt, *Akt*: The first term describes spontaneous *Akt* synthesis, the second one describes *Akt* dephosphorylation, the third and fourth terms represent *Akt* phosphorylation catalyzed by *ATMa* and *PIP3*, the fifth term represents *miR-145* inhibited *Akt* phosphorylation, while the last one stands for its spontaneous

degradation

$$\begin{aligned} \frac{d[Akt]}{dt} = & \sigma_d + k_{ed} \frac{[Akt_a]}{[Akt_a] + J_{ed}} - k_{ad} [ATMa] \frac{[Akt]}{[Akt] + J_{ad}} \\ & - k_{ud} [PIP3] \frac{[Akt]}{[Akt] + J_{ud}} - k_{id} \frac{[Akt]}{[miR-145] + J_{id}} \\ & - \delta_d [Akt] \end{aligned} \quad (S27)$$

Active Akt, *Akt_a*: The first two terms stand for *Akt* phosphorylation catalyzed by *ATMa* and *PIP3*, respectively, the third one describes *miR-145* inhibited *Akt* phosphorylation, and the next one represents *Akt_a* dephosphorylation, while the last one stands for its spontaneous degradation

$$\begin{aligned} \frac{d[Akt_a]}{dt} = & k_{ad} [ATMa] \frac{[Akt]}{[Akt] + J_{ad}} + k_{ud} [PIP3] \frac{[Akt]}{[Akt] + J_{ud}} \\ & + k_{id} \frac{[Akt]}{[miR-145] + J_{id}} - k_{ed} \frac{[Akt_a]}{[Akt_a] + J_{ed}} - \delta_e [Akt_a] \end{aligned} \quad (S28)$$

Inactive PIP3, *PIP2*: The first term stands for spontaneous *PIP2* synthesis, the second one describes *PIP3* dephosphorylation, the third term represents *PIP3* dephosphorylation catalyzed by *PTEN*, and the next one describes *PIP2* phosphorylation, while the last one stands for its spontaneous degradation

$$\begin{aligned} \frac{d[PIP2]}{dt} = & \sigma_w + k_{uw} \frac{[PIP3]}{[PIP3] + J_{uw}} + k_{tu} [PTEN] \frac{[PIP3]}{[PIP3] + J_{tu}} \\ & - k_{wu} \frac{[PIP2]}{[PIP2] + J_{wu}} - \delta_w [PIP2] \end{aligned} \quad (S29)$$

Active PIP3, *PIP3*: The first stem stands for *PIP2* phosphorylation, the second one describes *PIP3* dephosphorylation catalyzed by *PTEN*, the third stem represents *PIP3* spontaneous dephosphorylation, and the last one stands for its spontaneous degradation

$$\begin{aligned} \frac{d[PIP3]}{dt} = & k_{wu} \frac{[PIP2]}{[PIP2] + J_{wu}} - k_{tu} [PTEN] \frac{[PIP3]}{[PIP3] + J_{tu}} \\ & - k_{uw} \frac{[PIP3]}{[PIP3] + J_{uw}} - \delta_u [PIP3] \end{aligned} \quad (S30)$$

Active p21, *p21*: The first term describes spontaneous *p21* synthesis, the second term *p53a* driven *p21* synthesis, the next two terms describe *Myc* and *ARF* inhibited *p21* synthesis, respectively and the last one stands for its spontaneous degradation

$$\begin{aligned} \frac{d[p21]}{dt} = & \sigma_p + k_{cp} \frac{[p53a]^{np}}{[p53a]^{np} + J_{cp}^{np}} + k_{mp} \frac{J_{mp}^{na}}{[Myc]^{na} + J_{mp}^{na}} \\ & + k_{qp} \frac{J_{qp}^{nb}}{[ARF]^{nb} + J_{qp}^{nb}} - \delta_p [p21] \end{aligned} \quad (S31)$$

Active PTEN, *PTEN*: The first term describes spontaneous *PTEN* synthesis, the second one stands for *p53a* driven *PTEN* synthesis, and the next one represents its spontaneous degradation

$$\frac{d[PTEN]}{dt} = \sigma_t + k_{ct} \frac{[p53a]^{nt}}{[p53a]^{nt} + J_{ct}^{nt}} - \delta_t [PTEN] \quad (S32)$$

Active Siah-1, *Siah-1*: The first term describes spontaneous *Siah-1* synthesis, the second one stands for *p53a* driven *Siah-1* synthesis, and the next one represents its spontaneous degradation

$$\frac{d[Siah-1]}{dt} = \sigma_r + k_{cr} \frac{[P53a]^{nr}}{[P53a]^{nr} + J_{cr}^{nr}} - \delta_r [Siah-1] \quad (S33)$$

Active micro RNA 145, *miR-145*: The first term describes spontaneous *miR-145* synthesis, the second one stands for *p53a* driven *miR-145* synthesis, and the next one represents its spontaneous degradation

$$\frac{d[miR-145]}{dt} = \sigma_i + k_{ci} \frac{[p53a]^{ni}}{[p53a]^{ni} + J_{ci}^{ni}} - \delta_i [miR-145] \quad (S34)$$

Active P19/14ARF, *ARF*: The first stem stands for *ARF* spontaneous synthesis, the next four terms describe *betaC*, *Myc*, *Mucin1* and *p53* driven ARF synthesis, respectively, and the last one stands for its spontaneous degradation

$$\begin{aligned} \frac{d[ARF]}{dt} = & \sigma_q + k_{sq} \frac{[betaC]^{ns}}{[betaC]^{ns} + J_{sq}^{ns}} + k_{mq} \frac{[Myc]^{nm}}{[Myc]^{nm} + J_{mq}^{nm}} \\ & + k_{oq} \frac{[Mucin1]^{no}}{[Mucin1]^{no} + J_{oq}^{no}} + k_{cq} \frac{J_{cq}^{nc}}{[p53a]^{nc} + J_{cq}^{nc}} \\ & - \delta_q [ARF] \end{aligned} \quad (S35)$$

Active Beta-Catenin, *betaC*: The first stem stands for *betaC* spontaneous synthesis,

the second and third ones describe *p53* and *Siah-1* driven *betaC* degradation, respectively, the fourth one represents *Mucin1* inhibited *betaC* degradation, and the last one stands for its spontaneous degradation

$$\frac{d[\textit{betaC}]}{dt} = \sigma_s - k_{cs} [p53a] \frac{[\textit{betaC}]}{[\textit{betaC}] + J_{cs}} - k_{rs} [Siah-1] \frac{[\textit{betaC}]}{[\textit{betaC}] + J_{rs}} - k_{os} \frac{[\textit{betaC}]}{[Mucin1] + J_{os}} - \delta_s [\textit{betaC}] \quad (S36)$$

The definition of all the parameters in Eqs. (S1)- (S36) is shown in Table S2. The concentrations of all species are defined with respect to the total cell volume, which is assumed to $2 \times 10^{-6} \text{ m}^3$ and the mathematical models can explain and predict the behaviors of the molecules in dynamic equilibrium.

Table S2 Parameters, their descriptions and their numerical values

Parameter	Description	Units	Constant	Reference
kt	Rate of DSBs generation per time scale		0.01	1, 4
air	Number of DSBs generation per IR dose		35	1, 4
a1	Percentage of DSBs processed by fast repair		0.7	1, 4
a2	Percentage of DSBs processed by slow repair		0.3	1, 4
kdc1	Rate of DSBs transition to DSBCs in fast repair process		2	1, 4
kcd1	Rate of DSBCs transition to DSBs in fast repair process		0.5	1, 4
kdc2	Rate of DSBs transition to DSBCs in slow repair process		0.2	1, 4
kcd2	Rate of DSBCs transition to DSBs in slow repair process		0.05	1, 4
kcf1	Rate of DSBCs transition to Fixed DSB in fast repair process		0.001	1, 4
kcf2	Rate of DSBCs transition to F in slow repair process		0.0001	1, 4
kcross	Rate of DSB binary mismatch in second order repair process		0.001	1, 4
kundim	ATM undimerization rate		1	2
kdim	ATM dimerization rate		8	2
kaf	ATM phosphorylation rate		1	2
kar	ATM dephosphorylation rate		3	2
b1	Scale of the activation function of ATM phosphorylation		1	2
b2	Scale of the activation function of ATM		0.8	2

	phosphorylation			
b3	Scale of the activation function of ATM phosphorylation		0.08	2
Jab	Michaelis constant of ATMa-dependent p53 phosphorylation	μM	1	4
Jad	Michaelis constant of ATMa-dependent Akt phosphorylation	μM	0.1	5
Jah	Threshold concentration for ATMa-dependent Mdm2a degradation	μM	1.5	2
Jcb	Michaelis constant of p53a dephosphorylation	μM	0.1	4
Jcf	Michaelis constant of p53a-dependent mRNA-Mdm2 transcription	μM	1	2
Jci	Michaelis constant of p53a -dependent miR-145 transcription	μM	2	Estimated
Jcp	Michaelis constant of p53a –dependent p21 transcription	μM	2	Estimated
Jcq	Inhibition constant for repression of INK4a-ARF expression by p53a	μM	2	Estimated
Jcr	Michaelis constant of p53a -dependent Siah-1 transcription	μM	2	Estimated
Jcs	Threshold concentration for p53a-dependent Bate-Catenin degradation	μM	0.1	Estimated
Jct	Michaelis constant of p53a -dependent PTEN transcription	μM	2	5
Jed	Michaelis constant of Akta dephosphorylation	μM	0.1	5
Jeg	Michaelis constant of Akta-dependent Mdm2 phosphorylation	μM	0.3	5
Jhb	Threshold concentration for Mdm2a-dependent p53 degradation	μM	0.03	4
Jhc	Threshold concentration for Mdm2a-dependent p53a degradation	μM	0.3	4
Jhg	Michaelis constant of Mdm2a dephosphorylation	μM	0.1	5
Jid	Michaelis constant of miR-145-inhibition Akt phosphorylation	μM	0.1	Estimated
Jil	Michaelis constant of miR-145- inhibition mRNA-c-Myc translation	μM	0.5	Estimated
Jin	Michaelis constant of miR-145- inhibition mRNA-Mucin1 translation	μM	0.5	Estimated
Jjk	Michaelis constant of Cyclin E/cdk2 phosphorylation	μM	0.1	Estimated
Jkg	Michaelis constant of Cyclin E/cdk2a-inhibition Mdm2 phosphorylation	μM	0.1	Estimated
Jkj	Michaelis constant of Cyclin E/cdk2a dephosphorylation	μM	0.01	Estimated

				ed
Jmp	Inhibition constant for repression of p21 expression by c-Myc	μM	4	Estimated
Jmq	Michaelis constant of c-Myc-dependent INK4a-ARF transcription	μM	2	Estimated
Joq	Michaelis constant of Mucin1-dependent INK4a-ARF transcription	μM	2	Estimated
Jos	Threshold concentration for Mucin1-dependent Bate-Catenin degradation	μM	0.5	Estimated
Jpj	Michaelis constant of p21-dependent Cyclin E/cdk2a dephosphorylation	μM	0.1	Estimated
Jqh	Michaelis constant of p19/14ARF -dependent Mdm2a dephosphorylation	μM	0.1	Estimated
Jqp	Inhibition constant for repression of p21 expression by p19/14ARF	μM	4	Estimated
Jrs	Threshold concentration for Siah-1-dependent Bate-Catenin degradation	μM	0.1	Estimated
Jsq	Michaelis constant of Bate-Catenin-dependent INK4a-ARF transcription	μM	2	Estimated
Jtu	Michaelis constant of PTEN-dependent PIP3 dephosphorylation	μM	0.5	5
Jud	Michaelis constant of PIP3-dependent Akt phosphorylation	μM	0.1	5
Juw	Michaelis constant of PIP3 dephosphorylation	μM	0.1	5
Jwu	Michaelis constant of PIP2 Phosphorylation	μM	0.1	5
kab	ATMa-dependent phosphorylation rate of p53	$\mu\text{M}\cdot\text{m in}$	0.6	4
kad	ATMa-dependent phosphorylation rate of Akt	$\mu\text{M}\cdot\text{m in}$	0.1	5
kah	ATMa-dependent degradation rate of Mdm2a	$\mu\text{M}\cdot\text{m in}$	0.014	2
kcb	Dephosphorylation rate of p53a	$\mu\text{M}\cdot\text{m in}$	0.2	4
kcf	p53a-dependent transcription rate of mRNA-Mdm2	$\mu\text{M}\cdot\text{m in}$	0.024	2
kci	p53a-dependent miR-145 transcription rate	$\mu\text{M}\cdot\text{m in}$	0.01	Estimated
kcp	p53a-dependent p21 transcription rate	$\mu\text{M}\cdot\text{m in}$	0.01	Estimated
kcq	p53a-inhibition INK4a-ARF transcription rate	$\mu\text{M}\cdot\text{m in}$	0.024	Estimated
kcr	p53a-dependent Siah-1 transcription rate	$\mu\text{M}\cdot\text{m in}$	0.01	Estimated

kcs	p53a-dependent degradation rate of Bate-Catenin	$\mu\text{M}\cdot\text{m}$ in	1	Estimat ed
kct	p53a-dependent PTEN transcription rate	$\mu\text{M}\cdot\text{m}$ in	0.006	5
ked	Dephosphorylation rate of Akta	$\mu\text{M}\cdot\text{m}$ in	0.2	5
keg	Akta-dependent phosphorylation rate of Mdm2	$\mu\text{M}\cdot\text{m}$ in	10	5
kfg	Translation rate of mRNA-Mdm2	$\mu\text{M}\cdot\text{m}$ in	0.02	2
khh	Mdm2a-dependent degradation rate of p53	$\mu\text{M}\cdot\text{m}$ in	0.092	4
khc	Mdm2a-dependent degradation rate of p53a	$\mu\text{M}\cdot\text{m}$ in	0.018 4	4
khg	Dephosphorylation rate of Mdm2a	$\mu\text{M}\cdot\text{m}$ in	0.2	5
kid	miR-145-inhibition phosphorylation rate of Akt	$\mu\text{M}\cdot\text{m}$ in	0.045	Estimat ed
kil	miR-145- inhibition translation rate of mRNA-c-Myc	$\mu\text{M}\cdot\text{m}$ in	2	Estimat ed
kin	miR-145- inhibition translation rate of mRNA-Mucin1	$\mu\text{M}\cdot\text{m}$ in	0.5	Estimat ed
kjk	Phosphorylation rate of Cyclin E/cdk2	$\mu\text{M}\cdot\text{m}$ in	1.5	Estimat ed
kkg	Cyclin E/cdk2a -inhibition phosphorylation rate of Mdm2	$\mu\text{M}\cdot\text{m}$ in	0.01	Estimat ed
kkj	Dephosphorylation rate of Cyclin E/cdk2a	$\mu\text{M}\cdot\text{m}$ in	0.01	6
kmp	c-Myc-inhibition p21 transcription rate	$\mu\text{M}\cdot\text{m}$ in	0.01	Estimat ed
kmq	c-Myc-dependent INK4a-ARF transcription rate	$\mu\text{M}\cdot\text{m}$ in	0.1	Estimat ed
koq	Mucin1-dependent INK4a-ARF transcription rate	$\mu\text{M}\cdot\text{m}$ in	0.01	Estimat ed
kos	Muc1-dependent degradation rate of Bate-Catenin	$\mu\text{M}\cdot\text{m}$ in	10	Estimat ed
kpj	p21-dependent dephosphorylation rate of Cyclin E/cdk2a	$\mu\text{M}\cdot\text{m}$ in	2	Estimat ed
kqh	p19/14ARF -dependent dephosphorylation rate of Mdm2a	$\mu\text{M}\cdot\text{m}$ in	0.01	Estimat ed
kqp	p19/14ARF -inhibition p21 transcription rate	$\mu\text{M}\cdot\text{m}$ in	0.01	Estimat ed
krs	Siah-1-dependent degradation rate of Bate-Catenin	$\mu\text{M}\cdot\text{m}$	1	Estimat

ksq	Bate-Catenin-dependent INK4a-ARF transcription rate	$\mu\text{M}\cdot\text{m}$ in	0.01	Estimated
ktu	PTEN-dependent dephosphorylation rate of PIP3	$\mu\text{M}\cdot\text{m}$ in	73	5
kud	PIP3-dependent phosphorylation rate of Akt	$\mu\text{M}\cdot\text{m}$ in	20	5
kuw	Dephosphorylation rate of PIP3	$\mu\text{M}\cdot\text{m}$ in	0.1	5
kwu	Phosphorylation rate of PIP2	$\mu\text{M}\cdot\text{m}$ in	0.15	5
kxb	Translation rate of mRNA-p53	$\mu\text{M}\cdot\text{m}$ in	0.12	2
na	Degree of cooperativity of p21 expression by c-Myc	N/A	3	Estimated
nb	Degree of cooperativity of p21 expression by p19/14ARF	N/A	3	Estimated
nc	Degree of cooperativity of INK4a-ARF expression by p53a	N/A	3	Estimated
nf	Hill coefficient for mdm2 activation by p53a	N/A	4	2
ni	Hill coefficient for miR-145 activation by p53a	N/A	3	Estimated
nm	Hill coefficient for INK4a-ARF activation by c-Myc	N/A	3	Estimated
no	Hill coefficient for INK4a-ARF activation by Mucin1	N/A	3	Estimated
np	Hill coefficient for p21 activation by p53a	N/A	3	Estimated
nr	Hill coefficient for Siah-1 activation by p53a	N/A	3	Estimated
ns	Hill coefficient for INK4a-ARF activation by Bate-Catenin	N/A	3	Estimated
nt	Hill coefficient for PTEN activation by p53a	N/A	3	5
δb	Degradation rate of p53	min-1	0.02	2
δc	Degradation rate of p53a	min-1	0.008	4
δd	Degradation rate of Akt	min-1	0.01	Estimated
δe	Degradation rate of Akta	min-1	0.01	Estimated
δf	Degradation rate of mRNA-Mdm2	min-1	0.02	2
δg	Degradation rate of Mdm2	min-1	0.002 8	2
δh	Degradation rate of Mdm2a	min-1	0.002	Estimated

				ed
δi	Degradation rate of miR-145	min-1	0.01	Estimated
δj	Degradation rate of Cyclin E/cdk2	min-1	0.06	6
δk	Degradation rate of Cyclin E/cdk2a	min-1	0.05	6
δl	Degradation rate of mRNA-c-Myc	min-1	0.02	Estimated
δm	Degradation rate of c-Myc	min-1	0.034 7	Estimated
δn	Degradation rate of mRNA-Mucin1	min-1	0.02	Estimated
δo	Degradation rate of Mucin1	min-1	0.01	Estimated
δp	Degradation rate of p21	min-1	0.034 7	Estimated
δq	Degradation rate of p19/14ARF	min-1	0.05	Estimated
δr	Degradation rate of Siah-1	min-1	0.01	Estimated
δs	Degradation rate of Bate-Catenin	min-1	0.000 2	Estimated
δt	Degradation rate of PTEN	min-1	0.005 4	5
δu	Degradation rate of PIP3	min-1	0.001	5
δw	Degradation rate of PIP2	min-1	0.01	5
δx	Degradation rate of mRNA-p53	min-1	0.02	2
σd	Basal induction rate of Akt	$\mu M \cdot m$ in	0.01	Estimated
σf	Basal induction rate of mRNA-Mdm2	$\mu M \cdot m$ in	0.001 8	2
σi	Basal induction rate of miR-145	$\mu M \cdot m$ in	0.01	Estimated
σj	Basal induction rate of Cyclin E/cdk2	$\mu M \cdot m$ in	0.05	Estimated
σl	Basal induction rate of mRNA-c-Myc	$\mu M \cdot m$ in	0.002	Estimated
σn	Basal induction rate of mRNA-Mucin1	$\mu M \cdot m$ in	0.002	Estimated
σp	Basal induction rate of p21	$\mu M \cdot m$ in	0.02	Estimated
σq	Basal induction rate of p19/14ARF	$\mu M \cdot m$ in	0.01	Estimated
σr	Basal induction rate of Siah-1	$\mu M \cdot m$	0.01	Estimated

σ_s	Basal induction rate of Bate-Catenin	$\mu\text{M}\cdot\text{m}$ in	5	Estimated
σ_t	Basal induction rate of PTEN	$\mu\text{M}\cdot\text{m}$ in	0.001	5
σ_w	Basal induction rate of PIP2	$\mu\text{M}\cdot\text{m}$ in	0.02	Estimated
σ_x	Basal induction rate of mRNA-p53	$\mu\text{M}\cdot\text{m}$ in	0.02	2

Table S3 the raw data of the number of apoptosis cell for short-term simulation at various time points

		MCS																
		1	2	3	4	5	6	7	8	9	10	20	30	40	50	60	70	80
Group	1	2	3	5	6	7	10	11	11	11	11	11	11	11	12	12	12	12
	2	4	7	8	8	9	9	10	11	11	11	11	11	11	13	14	14	14
	3	1	2	3	3	5	5	9	11	11	11	11	11	12	13	13	13	13
	4	5	5	5	7	8	10	11	14	15	16	17	17	17	17	17	17	17
	5	1	4	7	9	10	10	11	11	12	12	12	12	12	13	13	13	13
	6	3	5	7	8	9	10	10	10	10	11	11	11	11	11	11	11	11
	7	3	4	5	7	9	10	12	12	12	12	12	12	12	12	12	12	12
	8	4	5	6	6	8	9	10	10	10	10	10	10	10	10	10	10	10
	9	1	3	7	8	10	12	14	14	15	15	16	16	17	17	17	17	17
	10	3	4	4	9	12	13	13	13	13	14	14	14	16	16	16	16	16
	11	2	3	7	10	10	12	16	16	16	17	17	17	17	18	18	18	18
	12	4	4	4	6	7	8	9	9	9	11	11	11	11	11	11	11	11
	13	1	3	5	6	8	11	11	11	12	12	12	13	13	13	14	14	14
	14	3	6	7	7	8	10	11	11	11	11	11	14	15	15	15	15	15
	15	2	8	8	10	11	11	12	12	12	12	12	12	12	12	12	12	12
	16	2	3	3	3	4	6	6	7	7	7	8	8	8	8	8	8	8
	17	2	2	4	7	7	8	8	10	11	11	12	12	12	13	13	13	13
	18	2	4	5	6	8	8	8	8	9	9	9	9	11	11	11	11	11
	19	3	3	4	4	5	5	7	9	9	10	10	10	10	10	10	10	10
	20	2	2	4	5	5	10	13	13	13	13	13	13	13	13	13	13	13
*		2.5	4	5.4	6.75	8	9.35	10.6	11.1	11.4	11.8	12	12.2	12.55	12.9	13	13	13
**		19.2	30.8	41.5	51.9	61.5	71.9	81.5	85.8	88.1	90.8	92.3	93.8	96.5	99.2	100	100	100

*: the average value of apoptosis cell

** : percentage of apoptosis cell (%)

Table S4 The raw data of the number of apoptosis cell in the loss regulative function system

Group	1	2	3	4	5	6	7	8	9	10
Number	75	79	72	82	83	79	75	71	76	83
Group	11	12	13	14	15	16	17	18	19	20
Number	81	76	78	80	75	83	81	79	73	75

for short-term simulation at 80 MCS time points.

Supplementary Figures

Figure S1 the dynamical behavior of p53 regulatory network molecules

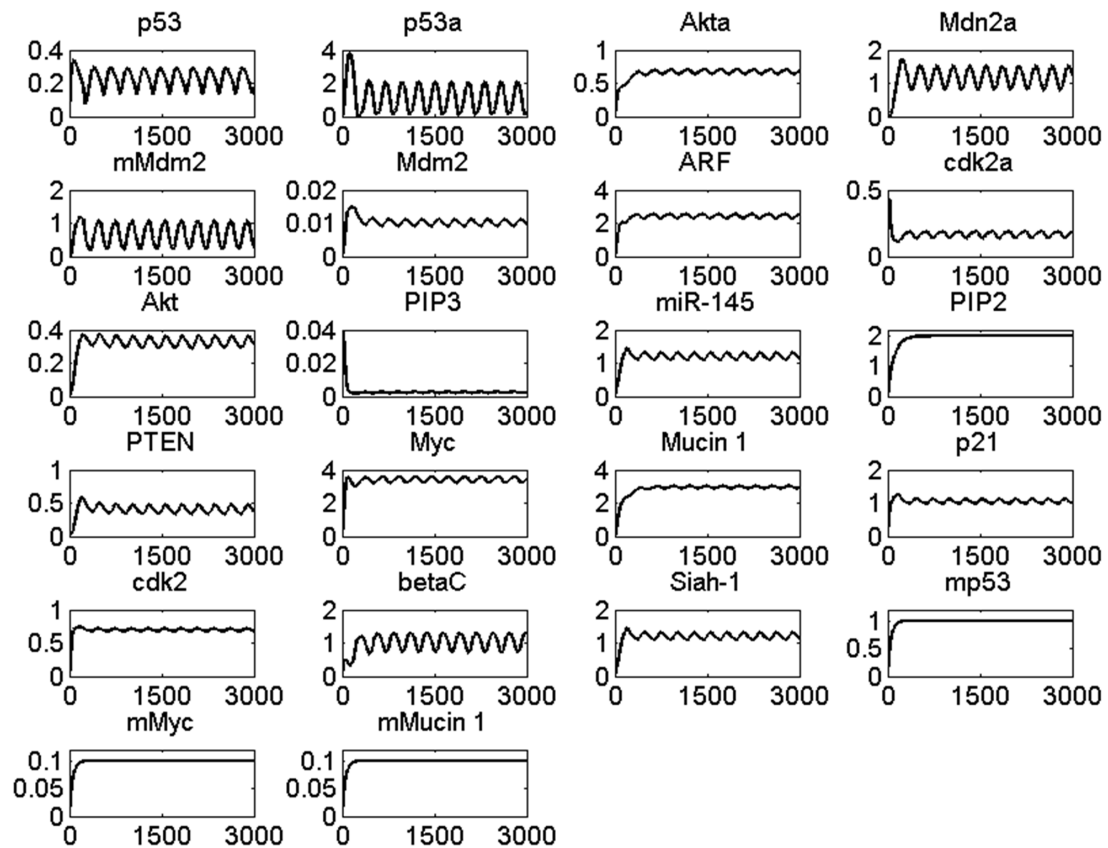


Fig. S1. The kinetics of p53 regulatory network system within 3000 min, the level of ATMa is fixed at the middle level for transforming zone ($ATMa = 1.73$). The time courses of 86% (19 for 22) molecules in the regulatory system undergo sustained oscillation with the same frequency and different swing.

Figure S2 The heat maps of local sensitivities of each reaction flux with respect to each parameter.

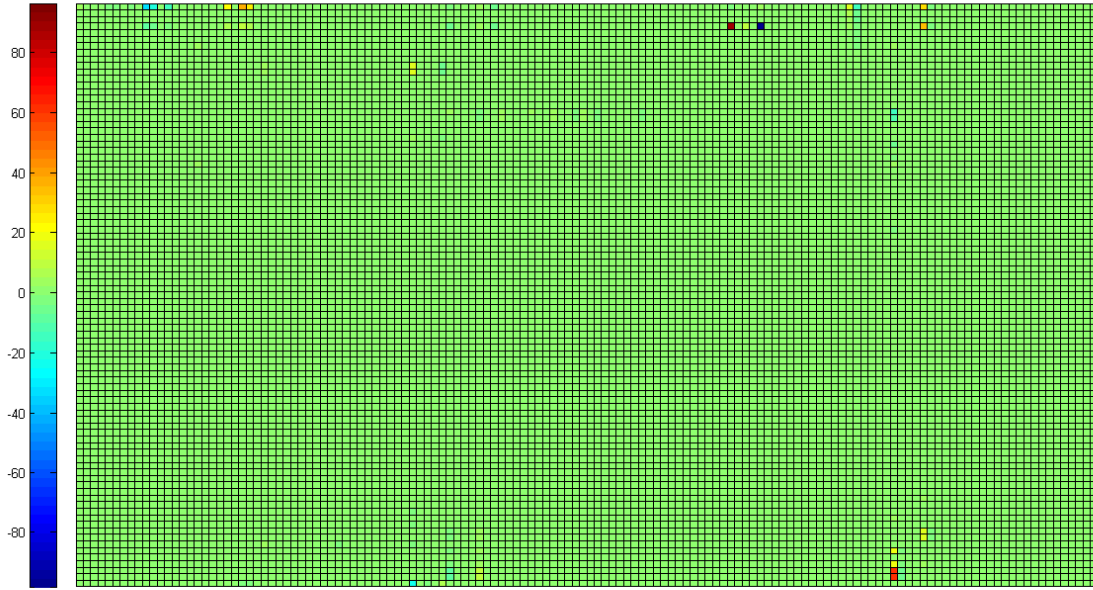


Fig. S2 The heat maps of local sensitivities of each reaction flux with respect to each parameter.

Each column represents a parameter, from left to right: k_{xb} , k_{ab} , J_{ab} , δ_b , δ_c , k_{hb} , J_{hb} , k_{hc} , J_{hc} , σ_f , k_{fg} , n_f , k_{cf} , J_{cf} , k_{ad} , J_{ad} , k_{qh} , J_{qh} , k_{kg} , J_{kg} , δ_f , δ_g , δ_h , k_{ah} , J_{ah} , σ_d , k_{eg} , J_{eg} , k_{ud} , J_{ud} , k_{id} , J_{id} , k_{ed} , J_{ed} , δ_d , δ_e , σ_w , k_{wu} , J_{wu} , k_{uw} , J_{uw} , k_{tu} , J_{tu} , δ_u , δ_w , σ_t , n_t , k_{ct} , J_{ct} , δ_t , σ_i , n_i , k_{ci} , J_{ci} , δ_i , δ_m , δ_o , σ_p , n_p , k_{cp} , J_{cp} , k_{mp} , J_{mp} , n_a , k_{qp} , J_{qp} , n_b , δ_p , σ_j , k_{jk} , J_{jk} , k_{kj} , J_{kj} , k_{pj} , J_{pj} , δ_k , δ_j , σ_q , n_s , k_{sq} , J_{sq} , n_m , k_{mq} , J_{mq} , n_o , k_{oq} , J_{oq} , δ_q , σ_r , n_r , k_{cr} , J_{cr} , δ_r , σ_s , δ_s , k_{cs} , J_{cs} , k_{rs} , J_{rs} , k_{os} , J_{os} , k_{cq} , J_{cq} , n_c , σ_x , δ_x , k_{cb} , J_{cb} , k_{hg} , J_{hg} , σ_l , δ_l , k_{il} , J_{il} , σ_n , δ_n , k_{in} , J_{in} , k_t , air , k_{cross} , b_1 , b_2 , b_3 , k_{af} , k_i , air , k_{cf1} , k_{cf2} , a_1 , a_2 , k_{cd1} , k_{cd2} , k_{dc1} , k_{dc2} , k_{ab} , J_{ab} , k_{ah} , J_{ah} , and each row represents a single reaction flux, from top to bottom: mRNA-p53 translation, p53 phosphorylation by ATMa, p53 degradation, p53a degradation, p53 degradation by Mdm2a, p53a degradation by Mdm2a, mMdm2 basal induction, mRNA-Mdm2 translation, mRNA-Mdm2 translation by p53a, Mdm2 phosphorylation by Akta, Mdm2a dephosphorylation by ARF, Mdm2 phosphorylation by cdk2a, mMdm2 degradation, Mdm2 degradation, Mdm2a degradation, Mdm2a degradation by ATMa, Akt basal induction, Akt phosphorylation by ATMa, Akt phosphorylation by PIP3, Akt phosphorylation by miR-145, Akta dephosphorylation, Akt degradation, Akta degradation, PIP2 basal induction, PIP2 phosphorylation, PIP3 dephosphorylation, PIP3 dephosphorylation by PTEN, PIP3 degradation, PIP2 degradation, PTEN basal induction, PTEN formation by p53a, PTEN degradation, miR-145 basal induction, miR-145 formation by p53a, miR-145 degradation, Myc degradation, Mucin1 degradation, p21 basal induction, p21 formation by p53a, p21 formation by Myc, p21 formation by ARF, p21 degradation, cdk2 basal induction, cdk2 phosphorylation, cdk2a dephosphorylation, cdk2a dephosphorylation by p21, cdk2a degradation, cdk2 degradation,

ARF basal induction, ARF transcription by betaC, ARF transcription by Myc, ARF transcription by Mucin1, ARF degradation, Siah-1 basal induction, Siah-1 formation by p53a, Siah-1 degradation, betaC basal induction, betaC degradation, betaC degradation by p53a, betaC degradation by Siah-1, betaC degradation by Mucin1, ARF formation by p53a, mRNA-p53 basal induction, mRNA-p53 degradation, p53a dephosphorylation, Mdm2a dephosphorylation, mRNA-Myc basal induction, mRNA-Myc degradation, Myc transcription by miR-145, mRNA-Mucin1 basal induction, mRNA-Mucin1 degradation, Mucin1 transcription by miR-145, DSBs generation, ATM undimerization, ATM dimerization, ATM dimerization, ATM phosphorylation, ATM dephosphorylation, DSBs generation, ATM undimerization, DSBCs1 transition to Fixed DSB1, DSBCs2 transition to Fixed DSB2, DSBs processed by fast repair, DSBs processed by slow repair, DSBCs1 transition to DSBs1, DSBCs2 transition to DSBs2, DSBs1 transition to DSBCs1, DSBs2 transition to DSBCs2, ATMa dephosphorylation by p53, ATMa dephosphorylation by Akt.

Figure S3 The heat map of 76 scaled sensitivity absolute values ($|S|$) for 44 parameters and 23 reactions >1 .

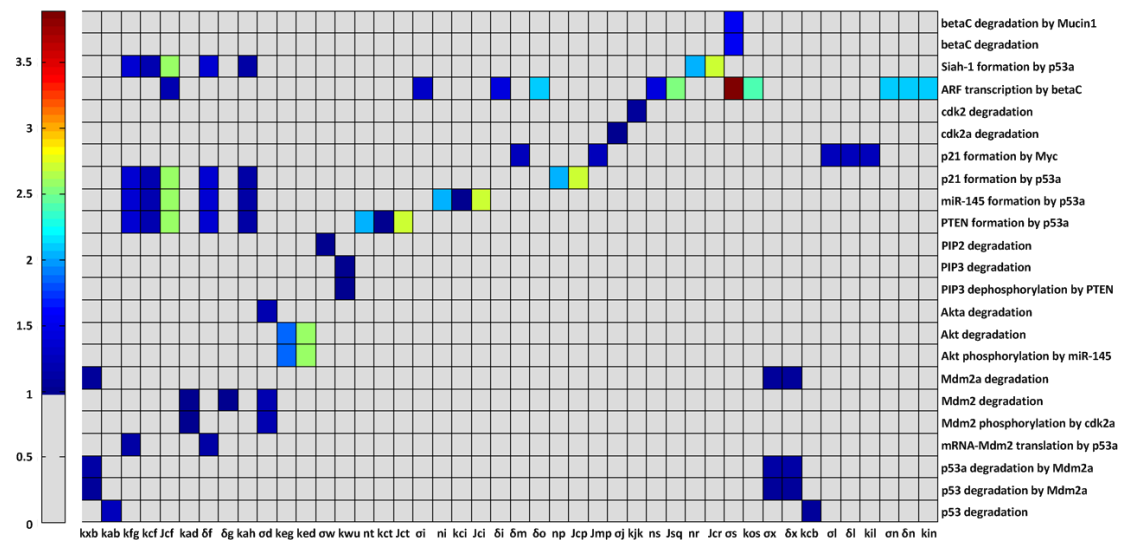


Fig. S3 The heat map of 76 scaled sensitivity absolute values ($|S|$) for 44 parameters and 23 reactions >1 in incomplete network without the p21 node. Each column represents a parameter, and each row represents a single reaction flux.

Figure S4 The normalized results of X_t in low and high steady state system

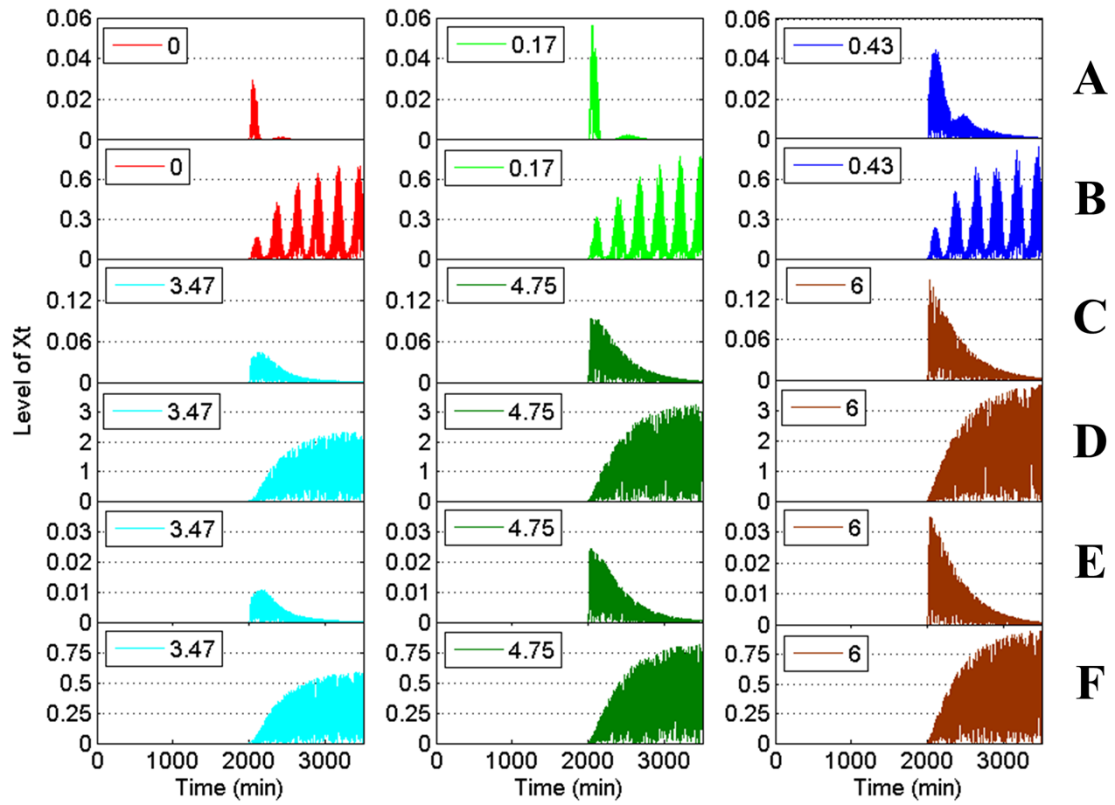


Fig. S4 The normalized results of X_t in low and high steady state system. (A), (C) and (E) the level of X_t for short-term stimulation; while (B), (D) and (F) for continuous stimulation. Red, green, blue, cyan, dark-green and brown line represent the level of X_t in 0, 0.17, 0.43, 3.47, 4.75 and 6 system, respectively. Here, the MinValue is 0; the MaxValue is 1500 in (A), (B), (C) and (D), while the MaxValue is 6000 in (E) and (F).

Figure S5 Plots showing snapshots of a sequence of the computation simulation results of the model at various time points

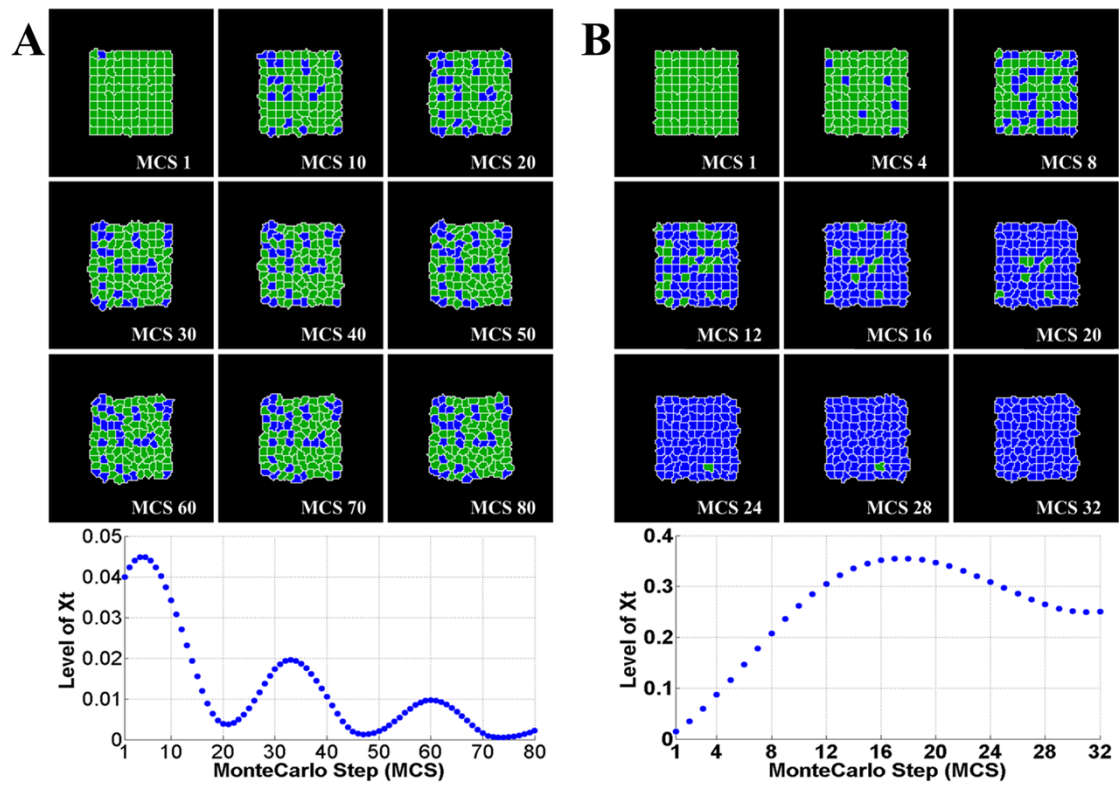


Fig. S5 Plots showing snapshots of a sequence of the computation simulation results of the model at various time points. (A) and (B) denote the plots of the spatial evolution of cell fate in low steady state (e.g., 1.73 system) under short-term and continuous stimulation, respectively. Colours of the cells correspond to state of cell, green and blue represent cell survival and apoptosis, respectively. Plots of X_t levels for the simulation in which cells undergo special treatments.

Figure S6a The snapshots of sequence of the computation simulation results of the $\text{MaxValue} = 1500$ in incomplete regulatory networks

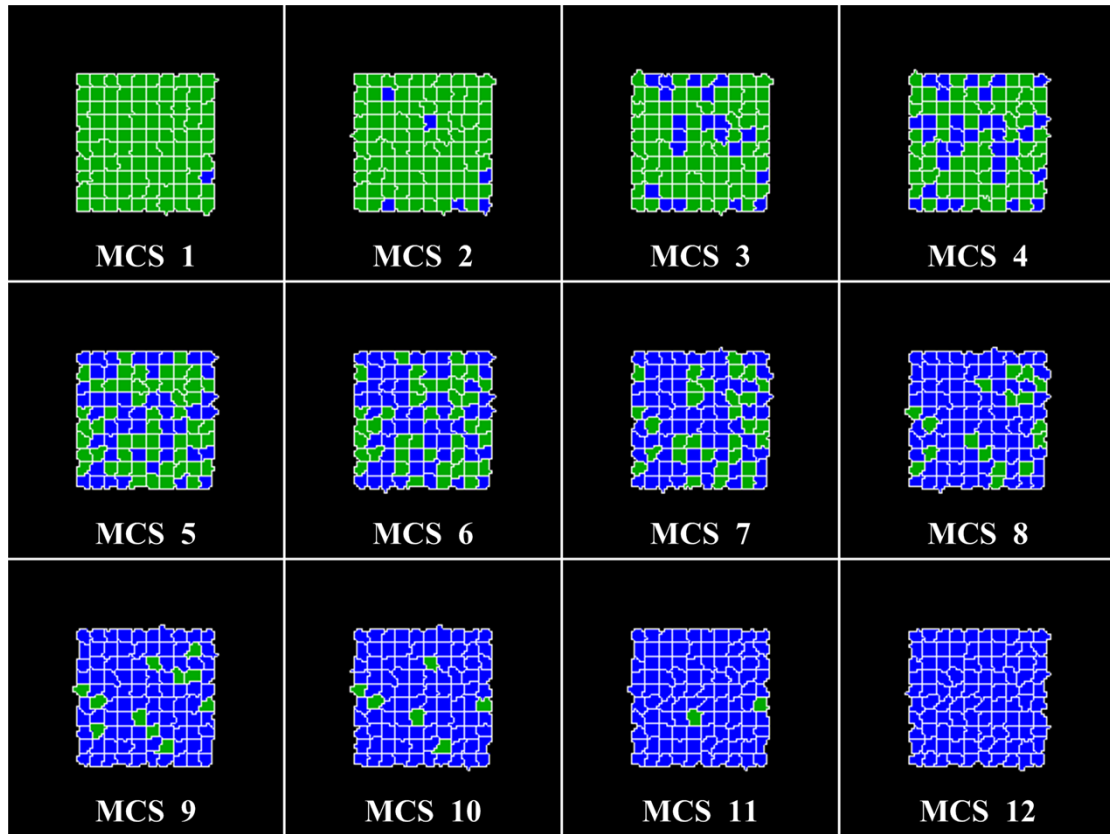
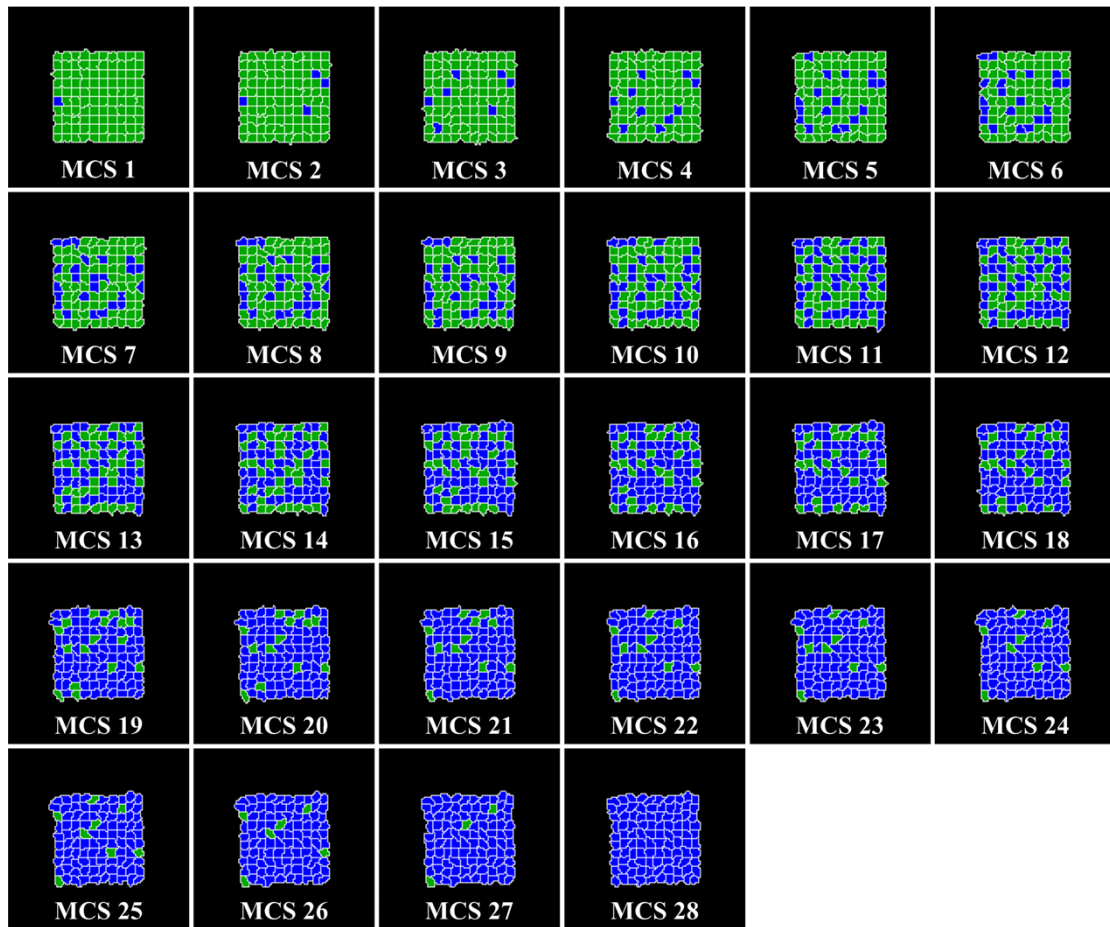


Figure S6b The snapshots of sequence of the computation simulation results of the $\text{MaxValue} = 8000$ in incomplete regulatory networks



References

1. G. Lahav, N. Rosenfeld, A. Sigal, N. Geva-Zatorsky, A. Levine, M. Elowitz and U. Alon, *Nature Genetics*, 2004, **36**, 147-150.
2. L. Ma, J. Wagner, J. Rice, W. Hu, A. Levine and G. Stolovitzky, *Proceedings of the National Academy of Sciences*, 2005, **102**, 14266.
3. J. Qi, Y. Ding and S. Shao, *Progress in Natural Science*, 2009, **19**, 1349-1356.
4. J. Qi, S. Shao, D. Li and G. Zhou, *Amino acids*, 2007, **33**, 75-83.
5. K. Wee and B. Aguda, *Biophysical journal*, 2006, **91**, 857-865.
6. M. Swat, A. Kel and H. Herzel, *Bioinformatics*, 2004, **20**, 1506.